Dynamics and thermodynamics of the spherical frustrated Blume-Emery-Griffiths model

A. Caiazzo, A. Coniglio, and M. Nicodemi
Dipartimento di Scienze Fisiche, INFM, Unitá di Napoli, Monte Sant'Angelo, I-80126 Napoli, Italy
(Received 5 June 2002; published 2 October 2002)

We introduce a spherical version of the frustrated Blume-Emery-Griffiths model and solve exactly the statics and the Langevin dynamics for zero particle-particle interaction ($K=0$). In this case the model exhibits an equilibrium transition from a disordered to a spin glass phase, which is always continuous for nonzero temperature. The same phase diagram results from the study of the dynamics. Furthermore, we note the existence of a nonequilibrium time regime in a region of the disordered phase, characterized by aging, as occurs in the glassy phase. Due to a finite equilibration time, the system displays in this region the pattern of interrupted aging.

DOI: 10.1103/PhysRevE.66.046101 PACS number(s): 05.50.+q, 75.10.Nr, 64.70.Pf, 64.60.Ht

I. INTRODUCTION

Many important features of spin glass models at mean field level have come out by studying their relaxional Langevin dynamics from a random initial condition [1–9]. The structure of the dynamical equations for the correlation and response functions has reaveled some analogies with other types of complex systems in which the disorder is *a priori* absent: at equilibrium the dynamics becomes formally identical to the mode coupling theory (MCT), which is the main approach to the supercooled liquids near the glass structural transition [10]. Thus there have been strong feelings that the two types of systems are deeply connected; in the glasses an effective disorder is self-induced by the slow dynamics of the microscopical variables [2].

For spin glass systems, the dynamical equations have been studied also in the low temperature phase [5–9]. These works provide a suggestion to extend the MCT below the glass temperature [11]. One of the main result has been that for these temperatures the system never reaches the equilibrium, but rather displays an off-equilibrium behavior where the dynamics depends on the whole history of the system up to the beginning of its observation and is characterized by the loss of validity of typical equilibrium properties, such as the time translational invariance (TTI) and the fluctuation-dissipation theorem (FDT). One can thus establish contact with some nonequilibrium experimental observations, namely, the slow relaxations and the aging phenomena which are observed for real spin glasses and many other complex systems [9].

Despite the cited resemblance, spin glasses are microscopically quite different from liquids and thus not suitable to their description. Recently, to make stronger connections with liquids, some models have been introduced which combine features of spin glasses and the lattice gas. Being constituted of particles, they allow to introduce the density and other related quantities which are usually important in the study of liquids. In this regard we consider the frustrated Blume-Emery-Griffiths (BEG) model [14,17], which is a quite general framework to describe different glassy systems. Its mean field Hamiltonian is

$$H=-\sum_{i<j} J_{ij}s_i n_i s_j n_j-\frac{K}{N}\sum_{i<j} n_i n_j-\mu\sum_i n_i, \qquad (1)$$

where $s_i=\pm 1$, $n_i=0,1$, μ is the chemical potential, and J_{ij} are quenched Gaussian interactions having zero mean and variance $[J_{ij}^2]_J=1/N$ [15]. Essentially the model consists of a lattice gas in a frustrated medium where the particles have an internal degree of freedom, given by their spin, which may account, as an example, of the possible orientations of complex molecules in glass forming systems. These steric effects are indeed greatly responsible for the geometric frustration appearing in glass forming systems at low temperatures or high densities. Besides that, the particles interact through a potential depending on the coupling K. In particular, for $K=0$ one recovers the Ghatak-Sherrington model [16] and for $K=-1$ the Ising frustrated lattice gas model [12]; this last case is related to the problem of the site frustrated percolation [22] and has also been used in the presence of gravity to describe granular materials [13]. However, as found by the standard replica theory [14,17], the model does not display substantial differences by varying K. The phase diagram in the plane μ-T shows a critical line separating a spin glass phase from a disordered one; the transition is continuous for large μ, as for the standard Ising spin glass ($n_i=1$), up to a given value μ_K^* below which it becomes discontinuous; in this region the Parisi solution has been obtained only recently in [17]. Moreover, a dynamical treatment of the model is still lacking.

We propose a spherical version of the frustrated BEG model, which allows a complete analysis of its equilibrium properties and even of Langevin dynamics. In this paper we study this model for $K=0$ leaving the general case to future investigations [18]. We find an equilibrium transition to a spin glass phase for $\mu\geqslant -1$, which is always continuous, like in the spherical SK model [19], except for $\mu=-1$ and $T=0$ (see Fig. 1). Furthermore, we investigate the Langevin dynamics of the various two-time functions and of density in the whole phase diagram. We get exact expressions of these quantities; they are, in general, rather complex, depending on several characteristic time scales whose number changes in the various regions of the phase diagram. In particular, the largest of these times is found to represent the characteristic equilibration time of the system, τ_{eq}. In the nonglassy phase this is finite and for waiting times $t'>\tau_{eq}$ the two-time functions obey TTI and FDT. This is no more true for $t'<\tau_{eq}$, the system being still out of equilibrium. By studying this regime near the critical line where τ_{eq} is large, we find two

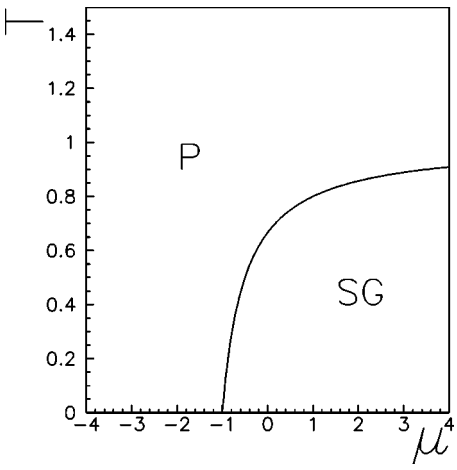

FIG. 1. The phase diagram T vs μ. The critical line separating the two phases is given by Eq. (6) for $\mu \geqslant -1$. The transition is always continuous except for the point $(\mu=-1, T=0)$.

different behaviors of the systems for $\mu > -1$ and $\mu \simeq -1$. We give here a first qualitative description of them. In the case $\mu > -1$ FDT still holds for $t - t' \ll t'$, so that deviations from the equilibrium case occur only for very small values of the correlation. Instead, as μ is close to -1, the range of correlation values in the FDT regime decreases and for $\mu = -1$ this vanishes; if t, t' are sufficiently lower than τ_{eq} the correlation function scales as a power of t'/t. Thus, in this region the observation of the system over short time scales could wrongly lead to conclude that the system is in the glassy phase. Then, for a large but finite τ_{eq}, the model follows the pattern of interrupted aging. Finally, τ_{eq} diverges in the whole glassy phase and the system displays essentially the same nonequilibrium behavior of the spherical SK model [7].

The paper is organized as follows. In Sec. II we define the spherical frustrated BEG model. In Sec. III we deal with the statics using the theory of large random matrices and analyze the thermodynamical properties. In Sec. IV we introduce the Langevin dynamical model and the various quantities of interest. In Sec. V we solve the integral equation related to the spherical constraints and compute the density. In Sec. VI we discuss the dynamics in the disordered phase and, after the identification of the equilibration time τ_{eq}, we analyze the equilibrium regime ($t' > \tau_{eq}$) and the out of equilibrium one ($t' < \tau_{eq}$). In Sec. VII we consider the nonequilibrium dynamics in the glassy phase ($\tau_{eq} = \infty$). Finally, in Sec. VIII we present some conclusions. Furthermore, in the Appendices A and B we study in detail, respectively, the equilibrium saddle point equation and the dynamics when this equation has degenere roots.

II. DEFINITION OF THE MODEL

First of all we note that the Hamiltonian (1) can be rewritten in terms of two new Ising spin fields $s_{1i}, s_{2i} = \pm 1$:

$$H = -\sum_{i<j} \frac{J_{ij}}{4}(s_{1i}+s_{2i})(s_{1j}+s_{2j}) - \frac{K}{4N}\sum_{i<j}(s_{1i}s_{2i}+1) \times (s_{1j}s_{2j}+1) - \frac{\mu}{2}\sum_{i}(s_{1i}s_{2i}+1), \tag{2}$$

where

$$s_{1i} = s_i, \quad s_i = s_{1i}, \quad \Leftrightarrow \quad s_{2i} = s_i(2n_i - 1), \quad n_i = \frac{1}{2}(s_{1i}s_{2i}+1), \tag{3}$$

[15]. The four-field interaction in Eq. (1) is replaced in Eq. (2) by four double field interactions; furthermore, the Hamiltonian (2) is symmetric under the exchange of the two spin fields. The overlap $q = [\langle s_i n_i \rangle^2]_J$ and the density $d = [\langle n_i \rangle]_J$, which are two usual order parameters for a diluted spin glass, now become, respectively, $\frac{1}{4}[\langle s_{1i} + s_{2i} \rangle^2]_J$ and $\frac{1}{2}[\langle s_{1i}s_{2i} \rangle + 1]_J$. So far we have just reformulated the BEG model. Now to define our spherical version, let the Ising constraints fall in Eq. (2) and replace them by the spherical ones: $\Sigma_i s_{1i}^2 = \Sigma_i s_{2i}^2 = N$. This particular choice of the variables to sphericize aims to obtain an exactly solvable model. It recovers the spherical SK model [19] in the large-μ limit ($s_{1i} = s_{2i}$). Below we will consider the case $K = 0$.

To study the model it is convenient to diagonalize the interaction matrix J_{ij} ($\Sigma_j J_{ij}\eta_{j\lambda} = \lambda \eta_{i\lambda}$) and work with the variables $s_{a\lambda} = \Sigma_i \eta_{i\lambda} s_{ai}$ ($a = 1,2$); these obey the properties $\Sigma_i s_{ai}s_{bi} = \Sigma_\lambda s_{a\lambda}s_{b\lambda}$ and $\Sigma_{ij} J_{ij} s_{ai}s_{bj} = \Sigma_\lambda \lambda s_{a\lambda}s_{b\lambda}$. In the $N \to \infty$ limit the eigenvalue density $\rho(\lambda)$ satisfies the Wigner semicircle law:

$$\rho(\lambda) = \begin{cases} \dfrac{1}{2\pi}\sqrt{4-\lambda^2}, & |\lambda| < 2 \\ 0, & |\lambda| \geqslant 2; \end{cases} \tag{4}$$

the quantities $\eta_{i\lambda}$ are Gaussian variables with zero mean and moments $[\eta_{i\lambda}^{2k}]_J = (2k-1)!!/N^k$; they are uncorrelated to the eigenvalues and among themselves, apart from the orthonormality and closure conditions.

III. EQUILIBRIUM PROPERTIES

A. Saddle point equation

The statics can be solved by standard techniques for spherical models and the above properties of large random matrices [19]. In the $N \to \infty$ limit the free energy is evaluated by steepest descent, by imposing saddle point conditions with respect to the two Lagrange multipliers z_1 and z_2, introduced by the spherical constraints. These equations just reproduce the two constraints satisfied on average, $\Sigma_\lambda \langle s_{a\lambda}^2 \rangle = N (a = 1,2)$. Explicitly they are reduced to only one:

$$\frac{1}{2\beta^2}[z - \sqrt{z^2 - 4\beta^2}] = 1 - \frac{1}{z + 2\beta\mu}, \tag{5}$$

where $z = z_1 + \beta\mu = z_2 + \beta\mu$ has to be greater than the branch points $\{2\beta, -2\beta\mu\}$. This condition is satisfied by a unique solution of Eq. (5), denoted by z_s, for each T if $\mu < -1$ and above a critical line, $T = T_c(\mu)$, for $\mu \geqslant -1$. This region of the phase diagram identifies the disordered phase

(labeled by P in Fig. 1). The critical line is located by z_s reaching the branch point 2β and is given by

$$T_c(\mu)=\frac{\mu+1}{\mu+3/2}. \tag{6}$$

A detailed study of Eq. (5) is given in Appendix A. Below the critical line (phase SG in Fig. 1) this equation is not satisfied for $z>2\beta$. The equilibrium saddle value of z sticks at the branch point 2β, and to preserve the spherical constraints a spontaneous magnetization arises along the eigenvector with eigenvalue 2. Actually, the diluted overlap $q=\frac{1}{4}[\langle s_{1i}+s_{2i}\rangle^2]_J$ is found to vanish when Eq. (5) holds and becomes just $\langle s_{a\lambda=2}\rangle^2/N$ below the critical line, i.e.,

$$q=1-\frac{1}{\beta}-\frac{1}{2(\beta+\beta\mu)}=1-\frac{T}{T_c(\mu)}. \tag{7}$$

The transition at the line $T=T_c(\mu)$ is continuous for each $\mu>-1$ and discontinuous at the point $(\mu=-1,T=0)$. Indeed the zero-temperature value of q is $\vartheta(\mu+1)$ with $q=0$ for $\mu=-1$. Note that the model could be solved using the replica trick, where a replica symmetric ansatz yields identical results.

B. Free energy and related quantities

The free energy per site f can be explicitly evaluated:

$$\beta f=\begin{cases} -\dfrac{z_s+2\beta\mu}{2}-\ln 4\pi+\dfrac{1}{2}\ln(z_s+2\beta\mu)+\dfrac{\beta^2}{4}\left(1-\dfrac{1}{z_s+2\beta\mu}\right)^2-\dfrac{1}{2}\ln\left(1-\dfrac{1}{z_s+2\beta\mu}\right), & \text{P} \\ -(\beta+\beta\mu)-\ln 4\pi+\dfrac{1}{2}\ln 2(\beta+\beta\mu)+\dfrac{1}{4}+\dfrac{1}{2}\ln\beta, & \text{SG;} \end{cases} \tag{8}$$

it corresponds to a negative low temperature entropy which diverges logarithmically as $T\to 0$. This pathology is typical of spherical models, even in the short-ranged uniform case.

Now we analyze other thermodynamic quantities in order to characterize the system and for comparison with the Ising case [14,17]. The density $d=\frac{1}{2}[\langle s_{1i}s_{2i}\rangle+1]_J$ is given by $-\partial f/\partial\mu$:

$$d=\begin{cases} 1-\dfrac{1}{z_s+2\beta\mu}, & \text{P} \\ 1-\dfrac{1}{2(\beta+\beta\mu)}, & \text{SG;} \end{cases} \tag{9}$$

it is represented in Fig. 2 as a function of T for several values of μ. In the large-temperature limit d approaches the value 1/2 for each μ. For $T=0$ we get $d=q=\vartheta(\mu+1)$ with $d=q=0$ for $\mu=-1$; note that, unlike the Ising version, there is no interval of μ values where $0<d<1$. In the spin glass phase a partial freezing takes place $(d<q<1)$, except at zero temperature where the system is fully frozen $(d=q=1)$. For $\mu\to\infty$ the model approaches the spherical SK limit [19]: $T_c=1$, $d=1$, $q=1-T$. The compressibility $k=(1/\beta)(\partial d/\partial\mu)$ is found to be

$$k=\begin{cases} \dfrac{2\left(1-\dfrac{1}{z_s+2\beta\mu}\right)}{(z_s+2\beta\mu)^2\left(1-\dfrac{1}{z_s+2\beta\mu}\right)+\sqrt{z_s^2-4\beta^2}}, & \text{P} \\ \dfrac{1}{2(\beta+\beta\mu)^2}, & \text{SG;} \end{cases} \tag{10}$$

its plot as a function of T is given in Fig. 3. A cusp at the critical temperature $T_c(\mu)$ whose height diverges in the limit $\mu\to-1^+$ is evident. k goes to the value 1/4 for each μ in the large temperature limit. For zero temperature $k=0$ for each μ. Finally the specific heat c is

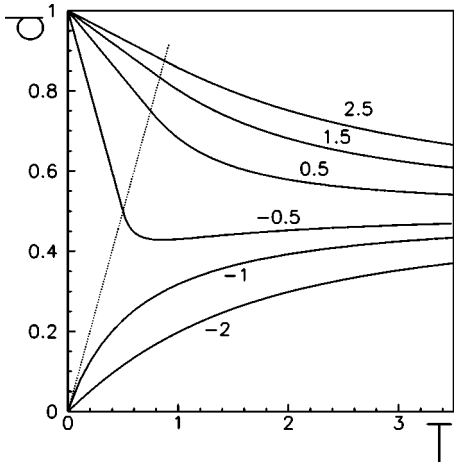

FIG. 2. The density d vs T for several values of μ. The intersection of the curves with the dotted line locates the critical temperature $T_c(\mu)$. Thus, the initial straight part of the curves for $\mu>-1$ corresponds to temperatures for which the system is in the glassy phase [bottom of Eq. (9)]. In the large-T limit d goes to the value 1/2 for each μ. Note also that at zero temperature $d=1$ for $\mu>-1$ and $d=0$ for $\mu\leqslant-1$.

$$c=\begin{cases} 1-\dfrac{z_s}{2}-\dfrac{\sqrt{z_s^2-4\beta^2}\left[(z_s+2\beta\mu)^2\left(1-\dfrac{1}{z_s+2\beta\mu}\right)+\beta\mu\right]-(z_s+2\beta\mu)^2}{(z_s+2\beta\mu)^2\left(1-\dfrac{1}{z_s+2\beta\mu}\right)+\sqrt{z_s^2-4\beta^2}}, & \text{P} \\ 1, & \text{SG;} \end{cases} \tag{11}$$

it presents a cusp at the transition for $\mu>-1$, while for $T=0$, it is discontinuous since $c=\frac{1}{2}$ for $\mu\leqslant -1$ (Fig. 4). The large-μ limit is given by $c=\frac{1}{2}+1/2T^2$ for $T>1$.

C. In the presence of a magnetic field

Adding to the Hamiltonian (2) a magnetic-field term, $-\Sigma_i(h_i/2)(s_{1i}+s_{2i})$, the saddle point equation is modified by adding $\int d\lambda\rho(\lambda)(\beta h_\lambda)^2/(z-\beta\lambda)^2$ to the left hand side of Eq. (5). Assuming a uniform field, $h_i=h$, one can replace h_λ^2 by its average value h^2. Thus one finds that for $h\neq 0$ there is no transition, since in this case z_s never reaches the branch point 2β.

Let us now compute the diluted susceptibilities in zero field. The linear one obeys the diluted Curie law in the disordered phase and is constant for $T<T_c(\mu)$, so to display a cusp crossing the critical line (Fig. 5):

$$\chi=-\frac{\partial^2 f}{\partial h^2}\Big|_{h=0}=\begin{cases} \beta\left(1-\dfrac{1}{z_s+2\beta\mu}\right), & \text{P} \\ 1, & \text{SG,} \end{cases} \tag{12}$$

notice that the previous result can be obtained also from the linear response theorem $\chi=\beta(d-q)$. The zero-temperature expression is $\chi=-\mu-\sqrt{\mu^2-1}$ for $\mu\leqslant -1$. The spin glass susceptibility is given by

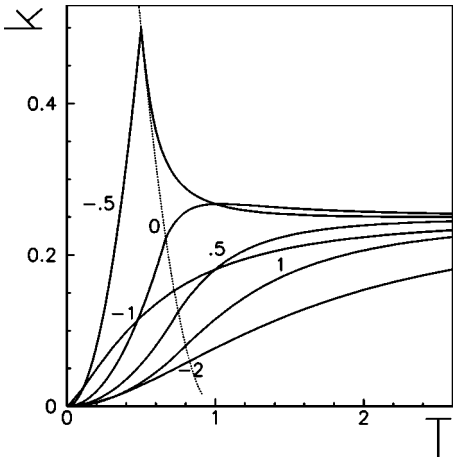

FIG. 3. The compressibility k vs T for several values of μ. A cusp is evident at the critical temperature $T_c(\mu)$ at least for values of μ close to -1. The height of the cusp diverges as $\mu\to -1^+$. The intersection of the dotted line with the curves for $\mu>-1$ locates the critical temperature $T_c(\mu)$; k increases with the square of T in the glassy phase [bottom of Eq. (10)]. For $T\to\infty$ k, goes to 1/4 for each μ.

$$\chi_{SG}=\sum_{\lambda\mu}\left(\frac{\partial^2 f}{\partial h_\lambda \partial h_\mu}\right)^2_{h=0}=\begin{cases} \dfrac{1}{2}\left(\dfrac{z_s}{\sqrt{z_s^2-4\beta^2}}-1\right), & \text{P} \\ \infty, & \text{SG;} \end{cases} \tag{13}$$

coming from high temperatures it diverges at the critical line as $1/[T-T_c(\mu)]$ and remains infinite in the whole frozen phase. For zero temperature it is given by $\chi_{SG}=\frac{1}{2}(-\mu/\sqrt{\mu^2-1}-1)$ for $\mu\leqslant -1$. The large-μ limit is $\chi_{SG}=1/T^2-1$ for $T>1$.

IV. LANGEVIN DYNAMICS

Now we deal with the Langevin relaxional dynamics of the model. Let us assume that the two spin fields evolve via usual Langevin equations, which when projected onto the basis λ become

$$\begin{aligned} \frac{ds_{1\lambda}}{dt}&=\left(\frac{\lambda}{4}-\frac{z_1(t)}{2}\right)s_{1\lambda}+\left(\frac{\lambda}{4}+\frac{\mu}{2}\right)s_{2\lambda}+h_{1\lambda}(t)+\xi_{1\lambda}(t) \\ \frac{ds_{2\lambda}}{dt}&=\left(\frac{\lambda}{4}+\frac{\mu}{2}\right)s_{1\lambda}+\left(\frac{\lambda}{4}-\frac{z_2(t)}{2}\right)s_{2\lambda}+h_{2\lambda}(t)+\xi_{2\lambda}(t), \end{aligned} \tag{14}$$

where $z_a(t)$, $a=1,2$ are two time-dependent Lagrange multipliers enforcing the spherical constraints, $h_{a\lambda}(t)$ are two

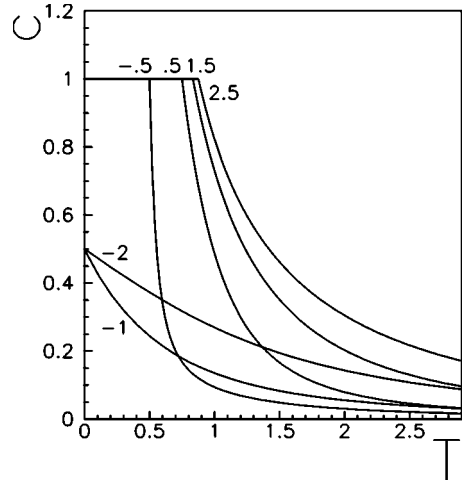

FIG. 4. The specific heat c vs T for several values of μ. Note the cusp at the transition temperature $T_c(\mu)$ for $\mu>-1$. $c=1$ in the glassy phase [bottom of Eq. (11)]. In the zero-T limit, $c=1/2$ for each $\mu\leqslant -1$.

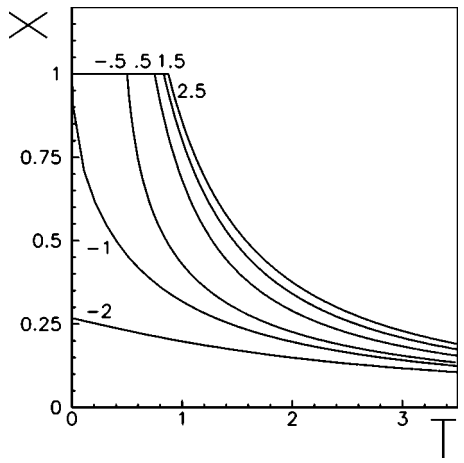

FIG. 5. The susceptibility χ vs T for several values of μ. Note the cusp at the transition temperature $T_c(\mu)$ for $\mu > -1$. $\chi = 1$ in the glassy phase [bottom of Eq. (12)]. In the zero-T limit $\chi = -\mu - \sqrt{\mu^2 - 1}$ for $\mu \leqslant -1$.

external fields interacting with the field $s_{a\lambda}$, and $\xi_{a\lambda}$ are the thermal noises with zero mean and correlations $\langle \xi_{a\lambda}(t)\xi_{b\mu}(t')\rangle = 2T\delta_{ab}\delta_{\lambda\mu}\delta(t-t')$, $a,b=1,2$. Hereafter we use $\langle\ \rangle$ to represent the average over the thermal noises.

Let us now introduce the quantities of interest, namely, the correlation functions $C_{ab}(t,t')$ $(a,b=1,2)$, the response functions $G_{ab}(t,t')$, and the density $d(t)$:

$$C_{ab}(t,t') = \left[\frac{1}{N}\sum_i \langle s_{ai}(t)s_{bi}(t')\rangle\right]_J = \int d\lambda\, \rho(\lambda)\langle s_{a\lambda}(t)s_{b\lambda}(t')\rangle, \tag{15}$$

$$G_{ab}(t,t') = \left[\frac{1}{N}\sum_i \left.\frac{\delta\langle s_{ai}(t)\rangle}{\delta h_{bi}(t')}\right|_{h=0}\right]_J = \int d\lambda\, \rho(\lambda)\left.\frac{\delta\langle s_{a\lambda}(t)\rangle}{\delta h_{b\lambda}(t')}\right|_{h=0}, \tag{16}$$

$$d(t) = \frac{1}{2}[C_{12}(t,t)+1]. \tag{17}$$

A quite general procedure allows one to derive from Eq. (14) closed equations for these functions as saddle point solutions of a dynamical generating functional [1,2]. Using this procedure one implicitly assumes the initial lattice fields $s_{ai}(0)$ as random variables with a Gaussian distribution of zero mean and variance $\overline{s_{ai}(0)s_{bi}(0)} = 1 + 2(1-\delta_{ab})[d(0) - 1]$ (the overbar stands for the average over the random initial conditions); the same is valid for $s_{a\lambda}(0)$, because of the rotational invariance of the Gaussian distribution. However, in our case these functional techniques can be avoided, as much as in Refs. [3,7]. Due to its linearity, the Langevin system (14) can be explicitely solved for given noises, thus the various dynamical quantities can be evaluated averaging over the noises and the eigenvalues λ. In the following we choose the initial conditions indicated previously. The dynamical model can be solved for any $d(0)$; but it can be shown that the value of $d(0)$ does not influence the long time behavior for nonzsero temperature, so we take for simplicity $d(0)=1$.

For zero external fields the dynamical model is for each time symmetric under the exchange of the two spin fields. Since below we will discuss the dynamics only in this case, we can exploit this symmetry and limit ourselves to solve Eqs. (14) for $z_1(t) = z_2(t)$. The solution is then given by

$$\begin{aligned} s_{a\lambda}(t) = \frac{1}{2\sqrt{\Gamma(t)}}\Big\{ & e^{\lambda t/2}[s_{1\lambda}(0)+s_{2\lambda}(0)] \\ & + \eta_a e^{-\mu t}[s_{1\lambda}(0)-s_{2\lambda}(0)] \\ & + \int_0^t du\, e^{\lambda(t-u)/2}\sqrt{\Gamma(u)}[\xi_{1\lambda}(u)+h_{1\lambda}(u)+\xi_{2\lambda}(u) \\ & + h_{2\lambda}(u)] + \eta_a\int_0^t du\, e^{-\mu(t-u)}\sqrt{\Gamma(u)} \\ & \times[\xi_{1\lambda}(u)+h_{1\lambda}(u)-\xi_{2\lambda}(u)-h_{2\lambda}(u)]\Big\}, \end{aligned} \tag{18}$$

where $\eta_a = \delta_{a,1} - \delta_{a,2}$ and

$$\Gamma(t) = \exp\int_0^t z(u)du, \quad z(t) = z_1(t) - \mu = z_2(t) - \mu. \tag{19}$$

As a consequence of the above symmetry, in the absence of external fields the four correlation functions coincide mutually, so we have to study only two of them: $C_{1a}(a=1,2)$. The same occurs for the relative response functions. Notice that when written in the original variables s_i and n_i, $C_{11}(t,t')$ is just the spin-spin correlation function, while $C_{12}(t,t')$ is a rather strange correlator made by a combination of spin and density variables. Instead, the density-density connected correlation function, which enters in the schematic version of MCT [20], involves 4-spin functions in the formalism of the lattice fields s_1, s_2:

$$C_{nn}(t,t') = \left[\frac{1}{4N}\sum_i [\langle s_{1i}(t)s_{2i}(t)s_{1i}(t')s_{2i}(t')\rangle - \langle s_{1i}(t)s_{2i}(t)\rangle\langle s_{1i}(t')s_{2i}(t')\rangle]\right]_J. \tag{20}$$

However, since the model is quadratic, this quantity is readily related to C_{1a} and we get $C_{nn}(t,t') = \frac{1}{4}[C_{11}(t,t')^2 + C_{12}(t,t')^2]$.

From Eq. (18), taking into account the previous initial conditions, we find for $t \geqslant t'$ and zero external fields

$$C_{1a}(t,t')=\frac{2}{\sqrt{\Gamma(t)\Gamma(t')}}\left[\frac{I_1(t+t')}{t+t'}+T\int_0^{t'}du\left(\frac{I_1(t+t'-2u)}{t+t'-2u}+\frac{\eta_a e^{-\mu(t+t'-2u)}}{2}\right)\Gamma(u)\right], \tag{21a}$$

$$G_{1a}(t,t')=\sqrt{\frac{\Gamma(t')}{\Gamma(t)}}\left[\frac{I_1(t-t')}{t-t'}+\frac{\eta_a}{2}e^{-\mu(t-t')}\right]. \tag{21b}$$

In these formulas I_1 is the modified Bessel function of order 1; we have used that $\int d\lambda\rho(\lambda)e^{\lambda t}=I_1(2t)/t$. Instead, the function $\Gamma(t)$ is still indeterminate; it can be computed self-consistently, as a solution of the integral equation obtained by enforcing the spherical constraint $C_{11}(t,t)=1$:

$$\Gamma(t)=\frac{I_1(2t)}{t}+T\int_0^t du\left[\frac{I_1(2(t-u))}{t-u}+e^{-2\mu(t-u)}\right]\Gamma(u). \tag{22}$$

Taking into account Eq. (22), one can get the following useful expressions for $C_{1a}(t,t')$ and $d(t)$:

$$C_{1a}(t,t')=\frac{\Gamma\left(\frac{t+t'}{2}\right)}{\sqrt{\Gamma(t)\Gamma(t')}}\left\{1+2\delta_{a,2}\left[d\left(\frac{t+t'}{2}\right)-1\right]-2T\int_{t'}^{(t+t')/2}du\left[\frac{I_1(t+t'-2u)}{t+t'-2u}+\frac{\eta_a}{2}e^{-\mu(t+t'-2u)}\right]\frac{\Gamma(u)}{\Gamma\left(\frac{t+t'}{2}\right)}\right\}, \tag{23a}$$

$$d(t)=1-\frac{T}{\Gamma(t)}\int_0^t du e^{-2\mu(t-u)}\Gamma(u). \tag{23b}$$

We note from these formulas that the behavior of $C_{1a}(t,t')$ at large times can be deduced from that of Γ and d; instead $d(t)$ takes contributions from Γ also at low times. However, we will be able to compute exactly $\Gamma(t)$ for each time and then also $d(t)$. In the limit $\mu\to\infty$ one can neglect the last term in Eqs. (21a)–(23b); hence $d(t)=1$, the two correlation functions and the two response functions coincide, recovering the case of the spherical SK model [7].

V. COMPUTING THE FUNCTION Γ AND THE DENSITY

First, we get $\Gamma(t)$ solving the integral equation (22) by Laplace transform techniques. Following [7], one could solve Eq. (22) using a suitable expansion which is valid in the spin glass phase. However, we proceed by a different technique in order to obtain $\Gamma(t)$ in the whole phase diagram. We find that the structure of the function $\Gamma(t)$ is related to the general roots of Eq. (5), discussed in detail in Appendix A.

Taking the Laplace transform of Eq. (22) and using the convolution theorem, after some algebra we put $\Gamma(s)$ in the form:

$$\Gamma(s)=\beta\left[\frac{P(\beta s)}{C(\beta s)}-\beta\frac{Q(\beta s)}{C(\beta s)}\left(\frac{s-\sqrt{s^2-4}}{2}\right)\right], \tag{24}$$

where $P(z)=(z+2\beta\mu)^2$, $Q(z)=(z+2\beta\mu)(z+2\beta\mu-1)$, and $C(z)$ is a third degree polynomial given by Eq. (A2). We see that $\Gamma(s)$ is written in terms of rational functions and $(s-\sqrt{s^2-4})/2$ which is the Laplace transform of $I_1(2t)/t$; thus in this form we can take readily the inverse transform. If $C(z)$ has distinct roots a_k $(k=1,2,3)$ this is given by

$$\Gamma(t)=\sum_{k=1}^{3}\left[\phi_k^P(a_k)e^{(a_k/\beta)t}-\beta\phi_k^Q(a_k)\int_0^t e^{(a_k/\beta)(t-u)}\frac{I_1(2u)}{u}du\right], \tag{25}$$

where $\phi_k^P(a_k)=P(a_k)/C'(a_k)$ and $\phi_k^Q(a_k)=Q(a_k)/C'(a_k)$ with $k=1,2,3$. The case of degenere roots (lines l_i in Fig. 8) can be treated analogously and presents no qualitative differences; so we leave it in Appendix B.

The integral appearing in Eq. (25) can be manipulated using the integral representation of the modified Bessel function I_1; we obtain

$$\int_0^t e^{-c\omega}\frac{I_1(\omega)}{\omega}d\omega=c-\sqrt{c^2-1}-e^{-(c-1)t}J_c(t),$$

$$J_c(t)=\frac{1}{\pi}\int_{-1}^{1}dx\frac{\sqrt{1-x^2}}{c-x}e^{(x-1)t}, \tag{26}$$

where c is, in general, complex but $\notin]-1,1[$. For long time the integral $J_c(t)$ can be evaluated analytically by a suitable expansion. For $t\gg 1/|c-1|$ we get

$$J_c(t)\simeq\frac{1}{\sqrt{2\pi t^3}(c-1)}\left[1-\frac{3}{2t}\left(\frac{1}{c-1}+\frac{1}{4}\right)\right]. \tag{27}$$

When c is real and close to 1, a new time regime exists for $1\ll t\ll 1/(c-1)$. In this regime we find a different behavior of the integral:

$$J_c(t)\simeq\sqrt{\frac{2}{\pi t}}\left[1-\sqrt{\pi t(c-1)}+2t(c-1)-\frac{1}{8t}\right]. \tag{28}$$

In particular, in the limit $c\to 1^+$ this regime holds for each $t\gg 1$ and one has $J_c(t)\simeq\sqrt{2/\pi t}$. Note that the leading term in Eq. (27) or Eq. (28) is enough for the following discussion; we retain the higher-order terms in the expansions only for the numerical calculations of the following section.

Let us come back to $\Gamma(t)$. Taking into account of Eq. (26), it can be rewritten as

$$\Gamma(t)=\sum_{k=1}^{3}\left[S(a_k)e^{(a_k/\beta)t}+\phi_k^Q(a_k)\beta e^{2t}J_{a_k/2\beta}(2t)\right], \tag{29}$$

where

$$S(a_k)=\phi_k^P(a_k)-\phi_k^Q(a_k)\left(\frac{a_k-\sqrt{a_k^2-4\beta^2}}{2}\right)=\begin{cases}\dfrac{(a_k+2\beta\mu)^2-\beta^2(a_k+2\beta\mu-1)^2}{C'(a_k)} & \text{if } a_k \text{ satisfies Eq. (5)}\\ \dfrac{C(a_k)}{C'(a_k)}=0 & \text{otherwise.}\end{cases} \tag{30}$$

Once $\Gamma(t)$ is known, the function $d(t)$ can be also exactly evaluated. Replacing Eq. (29) in Eq. (23b) we find

$$d(t)=1-\frac{T}{2\Gamma(t)}\sum_{k=1}^{3}\left\{\frac{S(a_k)}{a_k/2\beta+\mu}(e^{(a_k/\beta)t}-e^{-2\mu t})+\frac{\phi_k^Q(a_k)\beta}{a_k/2\beta+\mu}\left[e^{2t}[J_{a_k/2\beta}(2t)-J_{-\mu}(2t)]-e^{-2\mu t}\left(\frac{a_k-\sqrt{a_k^2-4\beta^2}}{2\beta}+\mu+\sqrt{\mu^2-1}\right)\right]\right\}. \tag{31}$$

From Eq. (30) we see that the exponentials with roots a_k not satisfying Eq. (5) play no role. To know what and how many exponentials make up $\Gamma(t)$ and $d(t)$ in the different regions of the phase diagram, one has just to consult the table (A5) and Fig. 8. Computing the large-time limit of $\Gamma(t)$ and $d(t)$, we find only a few different behaviors which we list now. For zero temperature we have $\Gamma(t)=I_1(2t)/t$ and $d(t)=1$ for each t and μ. In the spin glass phase and for $T=T_c(\mu)$ we retain in Eqs. (29) and (31) only the dominant exponential e^{2t}. Evaluating $J_{a_k/2\beta}(2t)$ and $J_{-\mu}(2t)$ by the leading term in Eq. (27), and then using the identity (A4), we get after some algebra

$$\Gamma(t)\simeq\frac{e^{2t}}{\sqrt{4\pi t^3}}\sum_{k=1}^{3}\frac{\beta^2\phi_k^Q(a_k)}{a_k-2\beta}=\frac{e^{2t}}{\sqrt{4\pi t^3}}\frac{d}{q_{EA}^2}, \tag{32a}$$

$$d(t)\simeq 1-\frac{T}{2\Gamma(t)}\sum_{k=1}^{3}\frac{\beta^2\phi_k^Q(a_k)}{a_k+2\beta\mu}\times\left[\frac{e^{2t}}{\sqrt{4\pi t^3}}\left(\frac{2\beta}{a_k-2\beta}+\frac{1}{\mu+1}\right)\right]=d, \tag{32b}$$

where q_{EA} is the Edwards-Anderson parameter coinciding with Eq. (7) and d is the equilibrium density given by the second part of Eq. (9). At the critical transition line, only a slight difference occurs with respect to the previous case: the integral $J_{a_1/2\beta}(2t)=J_1(2t)$, given by Eq. (28), prevails over the others for large t. Then using that $\phi_1^Q(2\beta)=1$ one has $\Gamma(t)\simeq\beta e^{2t}/\sqrt{\pi t}$. Finally, in the nonglassy phase we get readily $\Gamma(t)\simeq S(z_s)e^{(z_s/\beta)t}$, where z_s is the equilibrium solution of Eq. (5). Correspondingly, the density tends to its equilibrium value given by the top of Eq. (9).

VI. DYNAMICS IN THE NONGLASSY PHASE

Now we specialize the general expressions of the dynamical quantities obtained previously for the case of the nonglassy phase. It is convenient to put in evidence the large-time dominant exponential $e^{(z_s/\beta)t}$ in Eq. (29), $\Gamma(t)=e^{(z_s/\beta)t}\Omega(t)$,

$$\Omega(t)=S(z_s)+e^{-2t/\tau}\sum_{k=1}^{3}\beta\phi_k^Q(a_k)J_{a_k/2\beta}(2t)+e^{-2t/\tau_2}S(a_2)+e^{-2t/\tau_3}S(a_3) \tag{33}$$

and then replace $\Gamma(t)$ in Eqs. (23a), (23b) and (21b). We get the following exact expressions:

$$C_{1a}(t,t')=\frac{\Omega\left(\frac{t+t'}{2}\right)}{\sqrt{\Omega(t)\Omega(t')}}\left\{1+2\,\delta_{a,2}\left[d\left(\frac{t+t'}{2}\right)-1\right]-\frac{1}{\beta}\int_0^{t-t'}d\omega\left[\frac{I_1(\omega)}{\omega}e^{-\omega(1+1/\tau)}+\frac{\eta_a}{2}e^{-\omega/\tau'}\right]\frac{\Omega\left(\frac{t+t'-\omega}{2}\right)}{\Omega\left(\frac{t+t'}{2}\right)}\right\}, \tag{34a}$$

$$G_{1a}(t,t')=\sqrt{\frac{\Omega(t')}{\Omega(t)}}\left[\frac{I_1(t-t')}{t-t'}e^{-(t-t')(1+1/\tau)}+\frac{\eta_a}{2}e^{-(t-t')/\tau'}\right], \tag{34b}$$

$$d(t)=1-\frac{T}{2\Omega(t)}\left\{\frac{S(z_s)}{z_s/2\beta+\mu}(1-e^{-2t/\tau'})+\frac{S(a_2)}{a_2/2\beta+\mu}(e^{-2t/\tau_2}-e^{-2t/\tau'})+\frac{S(a_3)}{a_3/2\beta+\mu}\times(e^{-2t/\tau_3}-e^{-2t/\tau'})+\sum_{k=1}^{3}\frac{\phi_k^Q(a_k)\beta}{a_k/2\beta+\mu}\times\left[e^{-2t/\tau}[J_{a_k/2\beta}(2t)-J_{-\mu}(2t)]-e^{-2t/\tau'}\times\left(\frac{a_k-\sqrt{a_k^2-4\beta^2}}{2\beta}+\mu+\sqrt{\mu^2-1}\right)\right]\right\}. \tag{34c}$$

In the previous formulas we have introduced the

characteristic times:

$$\tau=\frac{1}{z_s/2\beta-1},\qquad \tau'=\frac{1}{z_s/2\beta+\mu},$$

$$\tau_2=\frac{1}{z_s/2\beta-a_2/2\beta},\qquad \tau_3=\frac{1}{z_s/2\beta-a_3/2\beta}. \tag{35}$$

We recall that the exponentials with the characteristic times τ_2,τ_3 are absent in the regions of the phase diagram, where the relative roots a_2,a_3 do not satisfy Eq. (5). In this regard see the table (A5) and Fig. 8.

A. Equilibrium dynamics

From the discussion done in Sec. III we deduce that τ_2 and τ_3, if present, are in any case lower than the largest between τ and τ'. This implies that the largest of the characteristic times (35) is given by $\tau_{eq}=\max\{\tau,\tau'\}$. In particular, one has $\tau_{eq}=\tau$ or τ' according to $\mu>-1$ or <-1, while for $\mu=-1$, $\tau_{eq}=\tau=\tau'$. The time τ_{eq} can be identified as the characteristic equilibration time of the system. In fact for waiting times $t'>\tau_{eq}$, the density (34c) is practically constant at the equilibrium value d given by the top of Eq. (9), while the two-time functions (34a),(34b) obey TTI and FDT ($TG_{1a}(t-t')=\partial C_{1a}(t-t')/\partial t'$), being given by

$$\begin{aligned}C_{1a}(t-t')&=1+2\,\delta_{a,2}(d-1)\\&\quad-\frac{1}{\beta}\int_0^{t-t'}d\omega\left[\frac{I_1(\omega)}{\omega}e^{-\omega(1+1/\tau)}+\frac{\eta_a}{2}e^{-\omega/\tau'}\right]\\&=e^{-(t-t')/\tau}\frac{J_{1+1/\tau}(t-t')}{\beta}+\frac{\eta_a\tau'}{2\beta}e^{-(t-t')/\tau'},\end{aligned} \tag{36a}$$

$$G_{1a}(t-t')=\frac{I_1(t-t')}{t-t'}e^{-(t-t')(1+1/\tau)}+\frac{\eta_a}{2}e^{-(t-t')/\tau'}. \tag{36b}$$

To obtain the second line we have used Eq. (26). Note that the equilibrium correlation functions $C_{1a}(t-t')$ decay exponentially to zero with the characteristic relaxation time given just by τ_{eq}. For $\mu>-1$, $\tau_{eq}=\tau$ diverges at the critical line, as $\tau\simeq 2T_c(\mu)^4/[T-T_c(\mu)]^2$, signaling critical slowing down; this implies that for each $\mu>-1$ the dynamical transition temperature coincides with the static one, as occurs in other continuous models [6–8]. Actually, the integral $J_{1+1/\tau}(t-t')$, given by Eq. (27) or Eq. (28), provides a power law correction to the exponential decay; it goes as $(t-t')^{-3/2}$ for $t-t'\gg\tau$ or as $(t-t')^{-1/2}$ in the critical regime for $t-t'\ll\tau$. Finally, τ_{eq} diverges also for $T\to 0$ and $\mu\leqslant -1$ as $\tau_{eq}=\tau'\simeq 2\beta$.

B. Nonequilibrium dynamics

For waiting times t' lower than τ_{eq} the system is not yet in equilibrium and the dynamics is described by Eqs. (34a)–(34c); these equations are formally analogous to those valid in the spin glass phase that we discuss below. When τ_{eq} is small, as usually occurs in the nonglassy phase, the equilibration is fast and the time range $t'<\tau_{eq}$ represents just a short initial transient. However, τ_{eq} can be made arbitrarily large as soon as one approaches the critical line, or for very low temperatures and $\mu\leqslant -1$; in such case a true nonequilibrium regime appears, although the system is in the nonglassy phase.

A quite useful way to characterize the relaxation process is by plotting the integrated response $\chi_{1a}(t,t')=\int_{t'}^{t}G_{1a}(t,u)du$, multiplied by the temperature T,

$$T\chi_{1a}(t,t')=\frac{1}{\beta}\int_0^{t-t'}d\omega\left[\frac{I_1(\omega)}{\omega}e^{-\omega(1+1/\tau)}+\frac{\eta_a}{2}e^{-\omega/\tau'}\right]\sqrt{\frac{\Omega(t-\omega)}{\Omega(t)}} \tag{37}$$

as a function of the correspondent correlation function $C_{1a}(t,t')$, given by Eq. (34a), for different values of t'. At equlibrium FDT implies a linear shape of these curves according to the relation $T\chi_{1a}=1+2\,\delta_{a,2}(d-1)-C_{1a}$, while this is no more true for $t'<\tau_{eq}$. We can thus analyze the changeover from the equilibrium to the nonequilibrium regime by monitoring how the curves deviate from this straight line. We find two different behaviors of the system along the critical line. In order to describe them, for simplicity we focus on the mode $a=1$.

For T close to $T_c(\mu)$ with μ not so close to the value -1 (see Fig. 1), one can readily show that for t large but sufficiently lower than τ_{eq} the function $\Omega(t)$ follows its critical behavior; one has indeed

$$\Omega(t)\simeq\beta\left(\sqrt{\frac{8}{\tau}}+e^{-2t/\tau}J_{1+1/\tau}(2t)\right),$$

so that $\Omega(t)\simeq\beta/\sqrt{\pi t}$ for $t\ll\tau/8\pi$, which is just the critical behavior. The time dependence of Ω would allow one to have aging in the correlation function. However, in this case the plot $T\chi_{11}$ vs C_{11} does not give much evidence of the nonequilibrium regime and we do not report it. In fact, for each $\mu>-1$ and finite temperature, even if $t,t'<\tau_{eq}$, FDT still holds when $t-t'\ll t'$: the function $C_{11}(t,t')$ follows its equilibrium expression (36a) and the plot starting out at the point $(C_{11}=1,T\chi_{11}=0)$ is linear again. If $t'\gg\tau'\simeq 1/(1+\mu)$, one has $C_{11}(t-t')\simeq 1/\beta\sqrt{2/\pi(t-t')}$ so that this regime extends up to small values of the correlation; thus small deviations from the straight line occur only in the last part of the plot until the end point $(C_{11}=0,T\chi_{11}=1)$ is asymptotically reached.

Instead, for low temperatures and μ near -1, the range of C_{11} values in the FDT regime $(t-t'\ll t')$ decreases and for zero temperature it disappears being $\chi_{11}=0$ for each t,t'. One finds for $\mu=-1$ and low T,

$$\Omega(t)\simeq\frac{1}{\beta}+e^{-2t/\tau}\frac{1}{\sqrt{4\pi t^3}},$$

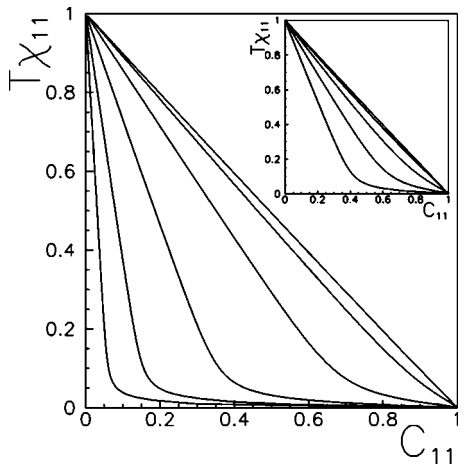

FIG. 6. $T\chi_{11}$ vs C_{11} for different values of t', with $\tau_{eq}\simeq 2\beta = 2\times 10^4$ and $\mu=-1$. We have taken $t'/\tau_{eq}=10^{-x}$ with $x=1,1.5,2,2.5,3,3.5$ for the curves, respectively, from the right to the left. The plot illustrates the nonlinear dependence of the integrated response $T\chi_{11}$ as a function of C_{11} when t' is lower than τ_{eq}. If the condition $t'/\tau_{eq}, t/\tau_{eq} \ll 1$ is realized, C_{11} obeys approximately the zero-temperature scaling form $2^{3/2}(t'/t)^{3/4}$ and χ_{11} is almost vanishing, as the system was in the low temperature glassy phase. The plot follows this shape for a range which is larger, the smaller the value of t'/τ_{eq} is. Then, as a consequence of the finite equilibration time, the plot must raise again in order to reach the point $(C_{11}=0, T\chi_{11}=1)$; thus the final upward bending of the curves corresponds to interrupted aging. The inset shows the curves obtained by keeping fixed $t'=50$ and varying μ around -1. We have taken $\mu=-1+10^{-x}$ with $x=2,2.5,3,3.5,4$ for the curves, respectively, from left to right. The initial straight part of the curves correspondent to the FDT regime increases with μ.

with $\tau=2\beta$; thus for $t\ll(\tau^2/16\pi)^{1/3}$ one recovers the zero-temperature behavior $\Omega(t)\simeq 1/\sqrt{4\pi t^3}$. It may also be shown that the same behavior occurs for $\mu<-1$ when $t\ll \ln\beta/2(-\mu-1)$. In Fig. 6 we show the curves $T\chi_{11}$ vs C_{11} for various t'/τ_{eq} obtained in the case $\mu=-1$ and low T so that $\tau_{eq}=2\times 10^4$. The model exhibits in this case the pattern of interrupted aging. If T is nonzero, i.e., $\tau_{eq}=2\beta$ is finite, the large-t limit of $C_{11}(t,t')$ and $T\chi_{11}$ is given, respectively, by 0 and 1. Therefore all the curves starting out at the point $(C_{11}=1, T\chi_{11}=0)$ must end up in the same point $(C_{11}=0, T\chi_{11}=1)$. The dependence on t'/τ_{eq} enters on how the initial and final point are joined. If $t'/\tau_{eq}>1$ a linear plot is obtained, as already said. If $t'/\tau_{eq}<1$, then the plot covers a very short part of the straight FDT line and then falls below this line. In particular, if the condition $t'/\tau_{eq}, t/\tau_{eq}\ll 1$ is realized, C_{11} obeys approximatively the zero-temperature scaling form $2^{3/2}(t'/t)^{3/4}$ and χ_{11} is almost vanishing. The plot follows this shape for a range which is larger, the smaller is the value of t'/τ_{eq}. Looking at these pieces of the curves only, one could wrongly conclude that the system is in the glassy phase. But, as t becomes larger than τ_{eq}, the plot must rise again in order to reach the point $(C_{11}=0, T\chi_{11}=1)$; thus the final upward bending of the curves is a consequence of a finite equilibration time and corresponds to interrupted aging. In the limiting case $\tau_{eq}=\infty$ aging holds for all time and the plot obeys $\chi_{11}=0$ over the entire range of C_{11} values. The behavior now described is similar to that recently found in the one-dimensional Ising model with Glauber dynamics [21], but in that case a less trivial shape of $T\chi(C)$ is obtained.

Finally, moving along or slightly above the critical line with $\mu\simeq -1$ for a fixed $t'=50$, one obtains the curves shown in the *inset* of Fig. 6. We note that their global shape is unchanged, but now the initial straight part corresponding to the FDT regime gets longer the larger μ.

VII. NONEQUILIBRIUM DYNAMICS IN THE GLASSY PHASE

The analysis of the nonequilibrium dynamics in the glassy phase is quite similar to that of the spherical SK model discussed in [7]. As above, we can put in evidence the dominant exponential in Eq. (29), which now is e^{2t}, and then replace $\Gamma(t)$ in Eqs. (23a), (23b) and (21b). The expressions we get for these quantities can be obtained by Eqs. (34a)–(34c) for $S(z_s)=0$ and

$$\tau=\infty, \quad \tau'=\frac{1}{1+\mu}, \quad \tau_2=\frac{1}{1-a_2/2\beta}, \quad \tau_3=\frac{1}{1-a_3/2\beta}. \tag{38}$$

The system is out of equilibrium on each time scale since τ_{eq} is infinite. Even if the roots a_2, a_3 satisfy Eq. (5), the characteristic times τ_2 and τ_3 are very small (lower than $\frac{1}{2}$) and, in practice, well inside the glassy phase, one has $\Omega(t)\simeq(1/\sqrt{4\pi t^3})(d/q_{EA}^2)$ and $d(t)\simeq d$, where q_{EA} is the Edwards-Anderson parameter coinciding with Eq. (7) and d the equilibrium density given by the bottom of Eq. (9). About the two-time quantities, for large times we distinguish the following two regimes.

(1) FDT regime for $t\simeq t'$ with $t-t'\ll t'$:

$$C_{1a}(t-t')=1+2\delta_{a,2}(d-1) - \frac{1}{\beta}\int_0^{t-t'} d\omega\left[\frac{I_1(\omega)}{\omega}e^{-\omega}+\frac{\eta_a e^{-\omega/\tau'}}{2}\right] = q_{EA}+\frac{J_1(t-t')}{\beta}+\frac{\eta_a\tau'}{2\beta}e^{-(t-t')/\tau'}, \tag{39a}$$

$$G_{1a}(t-t')=\frac{I_1(t-t')}{t-t'}e^{-(t-t')}+\frac{\eta_a}{2}e^{-(t-t')/\tau'}, \tag{39b}$$

where q_{EA} is the Edwards-Anderson parameter coinciding with Eq. (7) and d is the equilibrium density given by the bottom of Eq. (9). In this regime the properties TTI and FDT are satisfied. In the large $t-t'$ limit the two correlation functions have a power law decay to the value q_{EA} as $C_{1a}(t-t')-q_{EA}\simeq(1/\beta)\sqrt{2/\pi(t-t')}$; the reaching of q_{EA} determines the end of this regime.

(2) Aging regime for $t>t'$, $\lambda=t'/t\simeq 0$:

$$C_{1a}(t,t') = 2^{3/2}\frac{\lambda^{3/4}}{(1+\lambda)^{3/2}} q_{EA} \simeq 2^{3/2}\lambda^{3/4} q_{EA}, \quad (40a)$$

$$G_{1a}(t,t') = \frac{1}{\sqrt{2\pi}}\frac{\lambda^{-3/4}}{(1-\lambda)^{3/2}} t^{-3/2} \simeq \frac{1}{\sqrt{2\pi}}\lambda^{-3/4} t^{-3/2}. \quad (40b)$$

Here FDT and TTI are violated. The two correlation functions coincide and have a slow decay to zero obeying power scaling. For spin-glass-like models, in this regime FDT can be generalized to $TG(t,t') = X(C(t,t'))[\partial C(t,t')/\partial t']$, where X is the fluctuation-dissipation ratio assumed to depend on time arguments only through C and the function $X(C)$ is characteristic of the model [5–8]. In our case from Eqs. (40a),(40b) we get $X_{1a}(C_{1a}) = 0$, as in Ref. [7].

Figure 7 shows an example of plot $T\chi_{1a}$ vs C_{1a} obtained when the system in this phase. For larger t' the curves approach the asymptotes

$$T\chi_{1a} = \begin{cases} 1 + 2\delta_{a,2}(d-1) - C_{1a}, & q_{EA} < C_{1a} < 1 + 2\delta_{a,2}(d-1) \\ 1 + 2\delta_{a,2}(d-1) - q_{EA}, & 0 < C_{1a} < q_{EA}, \end{cases} \quad (41)$$

which can be derived by Eqs. (39a),(39b) and (40a),(40b); they correspond to the two regimes discussed previously. For zero temperature the FDT regime is absent ($q_{EA} = 1$).

VIII. CONCLUSIONS

We have defined a spherical version of the frustrated BEG model by enforcing spherical constraints to suitable Ising variables. The main advantage of such a model consists of its relative simplicity which allows to obtain a full analytical solution of the equilibrium properties and of Langevin relaxation dynamics at mean field level. As a first approach to the model, we have studied in detail the case $K = 0$, but the same kind of analysis can be equivalently carried out in the whole range of the parameter K [18].

Specifically, we have showed that quantities such as the density, the compressibility, or the density-density correlator, which are used in the study of liquids, can be introduced in this framework and exactly evaluated. This is convenient in the attempt to make a more suitable description of the glass transition, using the theoretical background developed for spin glasses. In this regard we note that the technique of sphericization used here could be applied and tested in other diluted spin glass models.

The equilibrium phase diagram, shown in Fig. 1, is rather simple. The line of discontinuous transition found in the Ising version of the model [14,17], in this spherical case with $K = 0$, collapses to a single point at $(\mu = -1, T = 0)$. Then the transition for $\mu > -1$ is always continuous, as occurs in the spherical SK model [19].

The study of the Langevin dynamics from a random initial condition has led to the same phase diagram. Nevertheless, this study has displayed a very interesting behavior. In the glassy phase it essentially reproduces the findings of [7] for the sperical SK model. Our exact analysis of the dynamics in the whole phase diagram has taken into account all the characteristic time scales of the system, which become important in the preasymptotic time regime. We have pointed out that a nonequilibrium regime, usually associated with the glassy phase, is possible also in the nonglassy phase for waiting times lower than the characteristic equilibration time. As for the glassy phase, it is characterized by a violation of FDT, manifested by a nonlinear behavior of the integrated response as a function of the correlation. In particular, we have seen that the presence of such nonequilibrium regime becomes more evident in the region near the point $(\mu = -1, T = 0)$, where the system displays explicitly the pattern of interrupted aging (Fig. 6). From an experimental or numerical point of view, this behavior could make rather ambigous the onset of the glassy phase if the system is probed on restricted time scales.

APPENDIX A: STUDY OF THE EQUILIBRIUM SADDLE POINT EQUATION

Here we carry out a detailed analysis of Eq. (5). The equilibrium solution z_s can be readily found in some simple limits. For $\mu \to \infty$ one can neglect in Eq. (5) the term $1/(z + 2\beta\mu)$ so as to recover the case of the spherical SK model [19] with solution $z_s = 1 + \beta^2$ for $T > 1$. In the limit T

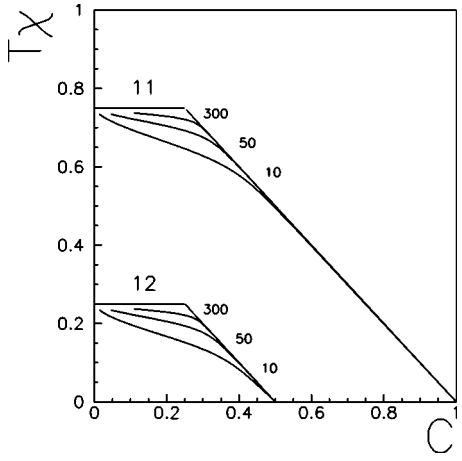

FIG. 7. $T\chi_{11}$ vs C_{11} and $T\chi_{12}$ vs C_{12} for different values of t', with $T = .5$ and $\mu = 0$. Notice that for larger t' the curve approaches the asymptotes given by Eq. (41), corresponding to the two large time regimes described in the text.

$\to T_c(\mu)^+$ we obtain at the leading order $z_s - 2/T_c(\mu) \simeq 1/T_c(\mu)^3[T/T_c(\mu)-1]^2$ with $\mu \neq -1$. Finally, a zero-temperature expansion gives $z_s \simeq -2\beta\mu + 1 + (-\mu - \sqrt{\mu^2-1})/\beta$ with $\mu \leqslant -1$.

Now we study Eq. (5) for z varying in the complex plane, since this is required during the discussion of the dynamics. Equation (5) is thus equivalent to

$$(z-2\beta)(z+2\beta) = f(z)^2, \quad f(z) = z - 2\beta^2\left(1 - \frac{1}{z+2\beta\mu}\right),$$

$$\arg(z-2\beta) + \arg(z+2\beta) = 2\arg f(z), \tag{A1}$$

with $\arg z \epsilon [0, 2\pi[$. The first of Eqs. (A1) gives rise to an equation of third degree:

$$C(z) = z^3 - A_2 z + A_1 z - A_0 = (z-a_1)(z-a_2)(z-a_3) = 0, \tag{A2}$$

where

$$A_2 = a_1 + a_2 + a_3 = 2 + \beta^2 - 4\beta\mu,$$

$$A_1 = a_1 a_2 + a_1 a_3 + a_2 a_3 = 4(\beta\mu)^2 - 6\beta\mu - 4\beta^3\mu + 2\beta^2, \tag{A3}$$

$$A_0 = a_1 a_2 a_3 = \beta^2(1-2\beta\mu)^2 + 4\beta^2\mu^2 > 0.$$

Furthermore, one can find the following identity:

$$(a_1 - 2\beta)(a_2 - 2\beta)(a_3 - 2\beta) = [2\beta(\beta+\beta\mu) - 2(\beta+\beta\mu) - \beta]^2 \geqslant 0. \tag{A4}$$

The previous relations can be used to get informations about the a_k corresponding to a given choice of T and μ. For example, from the zero-temperature expansion of z_s valid for $\mu \leqslant -1$, we obtain those of a_2, a_3: $a_2 \simeq -2\beta\mu + 1 + (-\mu + \sqrt{\mu^2-1})/\beta$, $a_3 \simeq \beta^2 + 2\mu/\beta$. However, in order to carry out a complete analysis of the possible a_k, we proceed solving Eq. (A2) numerically. Let us now give the results of our numerical calculations. The plane μ-T can be divided in various regions, as shown in Fig. 8. We have (1) a_1, a_2, a_3 real with $a_1, a_2, a_3 > 2\beta$ in the regions A_i $(i=1,2,3,4)$; (2) a_1 real, a_2, a_3 complex with $a_1 > 2\beta$ in the regions B_i $(i=1,2)$; (3) a_1, a_2, a_3 real with $a_1 > 2\beta$ and $a_2, a_3 < -2\beta$ in the regions C_i $(i=1,2,3,4)$.

Furthermore, in the point $Q = (-\sqrt{2}/2, \sqrt{2}/4)$ the three roots coincide: $a_1 = a_2 = a_3 = 6$. Along the lines l_i $(i=1,2,3,5,6)$ one has $a_2 = a_3$, while for l_4 and in the zero-temperature limit with $\mu \leqslant -1$: $a_1 = a_2$. In order to be a solution of Eq. (5) one a_k has to satisfy also the second of Eqs. (A1). Here is the list of such solutions in the various regions of the phase diagram:

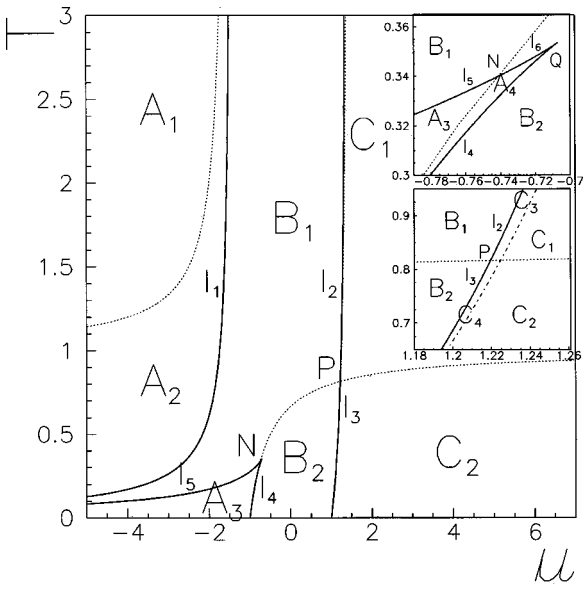

FIG. 8. The various regions of the plane μ-T with respect to the roots a_k $(k=1,2,3)$. The characteristics of the roots in the various regions are described in the text. The solid lines $(l_i i = 1, \ldots, 6)$ are defind by the vanishing of the discriminant of Eq. (A2), namely, $\frac{1}{4}(-\frac{2}{27}A_2 + \frac{1}{3}A_1A_2 - A_0)^2 + \frac{1}{27}(A_1 - \frac{1}{3}A_2^2)^3 = 0$. The dotted lines are given by Eq. (6) for $\mu < -1.5$ and $\mu \geqslant -1$. Finally, the dash-dotted line is given by $T = (1-\mu)/(\mu - 1.5)$ for $1 \leqslant \mu < 1.5$. The two insets show an enlargement of the regions around the point $N \simeq (-0.74, 0.34)$ and $P \simeq (1.22, 0.82)$. Notice, in particular, the existence of the very narrow regions A_4, C_3, C_4.

Regions	Solutions of Eq. (5)
C_3	$z_s > 2\beta, -2\beta\mu \; a_2, \quad a_3 < -2\beta, -2\beta\mu$
l_2	$z_s > 2\beta, -2\beta\mu \quad a_2 = a_3 < -2\beta, -2\beta\mu$
A_1	$z_s > 2\beta, -2\beta\mu \quad 2\beta < a_2 < -2\beta\mu$
C_1	$z_s > 2\beta, -2\beta\mu \quad a_2 < -2\beta, -2\beta\mu$
A_2, A_3, B_1, l_1, l_5	$z_s > 2\beta, -2\beta\mu$
C_4	$a_2, a_3 < -2\beta, -2\beta\mu$
l_3	$a_2 = a_3 < -2\beta, -2\beta\mu$
C_2	$a_2 < -2\beta, -2\beta\mu$
A_4, B_2, l_4, l_6	None

(A5)

APPENDIX B: COMPUTATION OF Γ AND OF THE DENSITY IN THE CASE OF DEGENERATE ROOTS

Here we discuss briefly the computation of the functions $\Gamma(t)$ and $d(t)$ when the third-degree polynomial $C(z)$ has no distinct roots (lines l_i in Fig. 8). Since the equilibrium solution z_s is never degenere, we do not find qualitative differences with respect to the no-degenerate case; in particular, the long time behaviors of Γ and d are unchanged.

First we consider the case of one doubly degenere root; let it be, for example, $a_2 = a_3$ and thus $C(z) = (z-a_1)(z-a_2)^2$. Computing the inverse transform of Eq. (24), Eq. (25) has to be replaced by

$$\Gamma(t)=\phi^P_{11}(a_1)e^{(a_1/\beta)t}-\beta\phi^Q_{11}(a_1)\int_0^t e^{(a_1/\beta)(t-u)}\frac{I_1(2u)}{u}du$$
$$+\phi^P_{21}(a_2)\frac{t}{\beta}e^{(a_2/\beta)t}-\beta\phi^Q_{21}(a_2)$$
$$\times\int_0^t e^{(a_2/\beta)(t-u)}\frac{(t-u)}{\beta}\frac{I_1(2u)}{u}du+\phi^P_{22}(a_2)e^{(a_2/\beta)t}$$
$$-\beta\phi^Q_{22}(a_2)\int_0^t e^{(a_2/\beta)(t-u)}\frac{I_1(2u)}{u}du, \tag{B1}$$

where $\phi^P_{11}(a_1)=P(a_1)/C'(a_1)$, $\phi^Q_{11}(a_1)=Q(a_1)/C'(a_1)$, $\phi^P_{2l}(a_2)=(d^{l-1}/dz^{l-1})[P(z)(z-a_2)^2/C(z)]|_{z=a_2}$, and $\phi^Q_{2l}(a_2)=(d^{l-1}/dz^{l-1})[Q(z)(z-a_2)^2/C(z)]|_{z=a_2}$ with $l=1,2$. Using the integral representation of the modified Bessel function I_1 we find

$$\Gamma(t)=e^{(a_1/\beta)t}S_1(a_1)+e^{(a_2/\beta)t}\left[\frac{t}{\beta}S_2(a_2)+S_2'(a_2)\right]$$
$$+e^{2t}\left[\beta\phi^Q_{11}(a_1)J_{1,a_1/2\beta}(2t)-\frac{1}{2}\phi^Q_{21}(a_2)J_{2,a_2/2\beta}(2t)\right.$$
$$\left.+\beta\phi^Q_{22}(a_2)J_{1,a_2/2\beta}(2t)\right] \tag{B2}$$

with $S_1(a_1)$ given by Eq. (30); furthermore,

$$S_2(a_2)=\phi^P_{21}(a_2)-\phi^Q_{21}(a_2)\left(\frac{a_2-\sqrt{a_2^2-4\beta^2}}{2}\right)=\begin{cases}[(a_2+2\beta\mu)^2-\beta^2(a_2+2\beta\mu-1)^2]\dfrac{1}{a_2-a_1} & \text{if } a_2 \text{ satisfies Eq. (5)}\\ \dfrac{C(a_2)}{a_2-a_1}=0 & \text{otherwise,}\end{cases} \tag{B3}$$

and the integrals $J_{k,c}(t)$ for $k=1,2$ are defined by

$$J_{k,c}(t)=\frac{1}{\pi}\int_{-1}^{1}\frac{\sqrt{1-x^2}}{(c-x)^k}e^{(x-1)t}dx. \tag{B4}$$

Notice that the integral $J_{1,c}(t)$ coincides with that defined by Eq. (26); furthermore, $J_{2,c}(t)$ is related to $J_{1,c}(t)$ by the relation $J_{2,c}(t)=-(\partial/\partial c)J_{1,c}(t)$. If a_2 does not satisfy Eq. (5), the whole coefficient of $e^{(a_2/\beta)t}$ vanishes since $C(a_2)=C'(a_2)=0$. The density is found to be

$$d(t)=1-\frac{T}{2\Gamma(t)}\left\{\frac{S(a_1)}{a_1/2\beta+\mu}(e^{(a_1/\beta)t}-e^{-2\mu t})+\frac{S_2(a_2)}{a_2/2\beta+\mu}\left[\frac{t}{\beta}e^{(a_2/\beta)t}-\frac{e^{(a_2/\beta)t}-e^{-2\mu t}}{2\beta(a_2/2\beta+\mu)}\right]\right.$$
$$+\frac{S_2'(a_2)}{a_2/2\beta+\mu}(e^{(a_2/\beta)t}-e^{-2\mu t})+\frac{\phi^Q_{11}(a_1)\beta}{a_1/2\beta+\mu}\{e^{2t}[J_{1,a_1/2\beta}(2t)-J_{1,-\mu}(2t)]-e^{-2\mu t}[\tilde{J}_{1,a_1/2\beta}-\tilde{J}_{1,-\mu}]\}$$
$$-\frac{\phi^Q_{21}(a_2)}{2(a_2/2\beta+\mu)}\left[e^{2t}\left(J_{2,a_2/2\beta}(2t)+\frac{J_{1,a_2/2\beta}(2t)-J_{1,-\mu}(2t)}{a_2/2\beta+\mu}\right)+e^{-2\mu t}\left(\tilde{J}_{2,a_2/2\beta}+\frac{\tilde{J}_{1,a_2/2\beta}-\tilde{J}_{1,-\mu}}{a_2/2\beta+\mu}\right)\right]$$
$$\left.+\frac{\phi^Q_{22}(a_2)\beta}{a_2/2\beta+\mu}\{e^{2t}[J_{1,a_2/2\beta}(2t)-J_{1,-\mu}(2t)]-e^{-2\mu t}[\tilde{J}_{1,a_2/2\beta}-\tilde{J}_{1,-\mu}]\}\right\}, \tag{B5}$$

where $\tilde{J}_{k,c}=J_{k,c}(0)$; one has, in particular, $\tilde{J}_{1,c}=c-\sqrt{c^2-1}$. We note that the long time behavior of $J_{k,c}(t)$ is given by $J_{k,c}(t)\simeq 1/\sqrt{2\pi t^3}(c-1)^k$; since it can be shown that

$$\frac{\beta^2\phi^Q_{11}(a_1)}{a_1-2\beta}-\frac{\beta^2\phi^Q_{21}(a_2)}{(a_2-2\beta)^2}+\frac{\beta^2\phi^Q_{22}(a_2)}{a_2-2\beta}=\frac{d}{q^2_{EA}},$$

one recovers the final results of the Eqs. (32a),(32b), valid in the spin glass phase.

Finally, let us consider the case $a_1=a_2=a_3$ (point Q in Fig. 8): $C(z)=(z-a_1)^3$. One has

$$\Gamma(t)=\sum_{l=1}^{3}\left[\frac{\phi_{3l}^{P}(a_1)}{(3-l)!(l-1)!}\left(\frac{t}{\beta}\right)^{3-l}+\frac{\beta\phi_{3l}^{Q}(a_1)}{(3-l)!(l-1)!}\int_0^t e^{(a_1/\beta)(t-u)}\left(\frac{t-u}{\beta}\right)^{3-l}\frac{I_1(2u)}{u}du\right], \tag{B6}$$

where $\phi_{3l}^{P}(a_1)=(d^{l-1}/dz^{l-1})P(z)|_{z=a_1}$, $\phi_{3l}^{Q}(a_1)=(d^{l-1}/dz^{l-1})Q(z)|_{z=a_1}$, $l=1,2,3$. Then, using the integral representation of I_1, one gets

$$\Gamma(t)=e^{(a_1/\beta)t}\left[\frac{1}{2}\left(\frac{t}{\beta}\right)^2 S(a_1)+\left(\frac{t}{\beta}\right)S'(a_1)+\frac{1}{2}S''(a_1)\right]+e^{2t}\left[\frac{\phi_{31}^{Q}(a_1)}{4\beta}J_{3,a_1/2\beta}(2t)-\frac{1}{2}\phi_{32}^{Q}(a_1)J_{2,a_1/2\beta}(2t)\right.$$
$$\left.+\frac{1}{2}\beta\phi_{33}^{Q}(a_2)J_{1,a_1/2\beta}(2t)\right], \tag{B7}$$

where

$$S(a_1)=\phi_{31}^{P}(a_1)-\phi_{31}^{Q}(a_1)\left(\frac{a_1-\sqrt{a_1^2-4\beta^2}}{2}\right)=\begin{cases}(a_1+2\beta\mu)^2-\beta^2(a_1+2\beta\mu-1)^2 & \text{if } a_1 \text{ satisfies Eq. (5)}\\ C(a_1)=0 & \text{otherwise,}\end{cases} \tag{B8}$$

and the integrals $J_{k,c}(t)$ are defined by Eq. (B4) for $k=1,2,3$. In particular, one has $J_{3,c}(t)=\frac{1}{2}(\partial^2/\partial c^2)J_{1,c}(t)$. The coefficient of $e^{(a_1/\beta)t}$ vanishes since $C(a_1)=C'(a_1)=C''(a_1)=0$. The density is

$$d(t)=1-\frac{T}{2\Gamma(t)}\left\{\frac{\phi_{31}^{Q}(a_1)}{4\beta(a_1/2\beta+\mu)}\left[e^{2t}\left(J_{3,a_1/2\beta}(2t)+\frac{J_{2,a_1/2\beta}(2t)}{a_1/2\beta+\mu}+\frac{J_{1,a_1/2\beta}(2t)-J_{1,-\mu}(2t)}{(a_1/2\beta+\mu)^2}\right)\right.\right.$$
$$\left.+e^{-2\mu t}\left(\tilde{J}_{3,a_1/2\beta}+\frac{\tilde{J}_{2,a_1/2\beta}}{a_1/2\beta+\mu}+\frac{\tilde{J}_{1,a_1/2\beta}-\tilde{J}_{1,-\mu}}{(a_1/2\beta+\mu)^2}\right)\right]-\frac{\phi_{32}^{Q}(a_1)}{2(a_1/2\beta+\mu)}\left[e^{2t}\left(J_{2,a_1/2\beta}(2t)+\frac{J_{1,a_1/2\beta}(2t)-J_{1,-\mu}(2t)}{a_1/2\beta+\mu}\right)\right.$$
$$\left.\left.+e^{-2\mu t}\left(\tilde{J}_{2,a_1/2\beta}+\frac{\tilde{J}_{1,a_1/2\beta}-\tilde{J}_{1,-\mu}}{a_1/2\beta+\mu}\right)\right]+\frac{\phi_{33}^{Q}(a_1)\beta}{2(a_1/2\beta+\mu)}\{e^{2t}[J_{1,a_1/2\beta}(2t)-J_{1,-\mu}(2t)]-e^{-2\mu t}(\tilde{J}_{1,a_1/2\beta}-\tilde{J}_{1,-\mu})\}\right\}, \tag{B9}$$

where $\tilde{J}_{k,c}=J_{k,c}(0)$. From $J_{k,c}(t)\simeq 1/\sqrt{2\pi t^3(c-1)^k}$ and

$$\frac{1}{2}\frac{\beta^2\phi_{33}^{Q}(a_1)}{a_1-2\beta}-\frac{\beta^2\phi_{32}^{Q}(a_1)}{(a_1-2\beta)^2}+\frac{\beta^2\phi_{31}^{Q}(a_1)}{(a_1-2\beta)^3}=\frac{d}{q_{EA}^2}$$

one gets again the final results of Eqs. (32a),(32b), valid in the spin glass phase.

[1] H. Sompolinsky and A. Zippelius, Phys. Rev. B **25**, 6860 (1982).

[2] T.R. Kirkpatrick and D. Thiumalai, Phys. Rev. B **36**, 5388 (1987); Phys. Rev. Lett. **58**, 2091 (1987).

[3] S. Ciuchi and F. De Pasquale, Nucl. Phys. B **300(FS22)**, 31 (1988).

[4] A. Crisanti, H. Horner, and H.-J. Sommers, Z. Phys. B: Condens. Matter **92**, 257 (1993).

[5] L.F. Cugliandolo and J. Kurchan, Phys. Rev. Lett. **71**, 173 (1993).

[6] L.F. Cugliandolo and J. Kurchan, J. Phys. A **27**, 5749 (1994).

[7] L.F. Cugliandolo and D.S. Dean, J. Phys. A **28**, 4213 (1995).

[8] L.F. Cugliandolo and P. Le Doussal, Phys. Rev. E **53**, 1525 (1996).

[9] J.P. Bouchaud, L.F. Cugliandolo, J. Kurchan and Mezard M., *Out of Equilibrium Dynamics in Spin Glasses and Other Glassy Systems in Spin Glasses and Random Fields*, edited by A. P. Young (World Scientific, Singapore, 1997).

[10] W. Gotze, in *Liquids, Freezing and Glass Transition*, 1989 Les Houches Lectures, edited by J. P. Hansen, D. Levesque, Zinn-Justin (North-Holland, Amsterdam, 1991).

[11] J.P. Bouchaud, L.F. Cugliandolo, J. Kurchan and M. Mezard, Physica A **226**, 243 (1996).

[12] M. Nicodemi and A. Coniglio, J. Phys. A **30**, L187 (1997); J. Arenzon, M. Nicodemi, and M. Sellitto, J. Phys. I **6**, 1143 (1996); A. Coniglio, A. de Candia, A. Fierro, and M. Nicodemi, J. Phys.: Condens. Matter **11**, A167 (1999).

[13] M. Nicodemi, A. Coniglio and H.J. Herrmann, Phys. Rev. E **55**, 3962 (1997); A. Coniglio and M. Nicodemi, Phys. Rev. Lett. **82**, 916 (1999); M. Nicodemi, *ibid.* **82**, 3734 (1999); A. Coniglio and M. Nicodemi, J. Phys.: Condens. Matter **12**, 6601 (2000).

[14] M. Sellitto, M. Nicodemi, and J. Arenzon, J. Phys. I **7**, 945 (1997); G.R. Shreiber, Eur. Phys. J B **9**, 479 (1999).

[15] As static properties are concerned, the two Ising lattice fields s_i, n_i can be replaced by the single spin-1 field $\tau_i = s_i n_i = 0, \pm 1$ apart from a simple rescaling of μ. The change of variables in Eq. (3) is rewritten in terms of τ_i as $\tau_i = (s_1 i + s_2 i)/2$.

[16] S.K. Ghatak and D. Sherrington, J. Phys. C **10**, 3149 (1977); E.J.S. Large and J.R.L. de Almeida, *ibid.* **15**, L1187 (1982); P. Mottishaw and D. Sherrington, *ibid.* **18**, 5201 (1985); F.A. de Costa, C.S.O. Yokoi, and S.R. Salinas, J. Phys. A **27**, 3365 (1994).

[17] A. Crisanti and L. Leuzzi, e-print cond-mat/0204349.

[18] A. Caiazzo, A. Coniglio, and M. Nicodemi (in preparation).

[19] J.M. Kosterlitz, D.J. Thouless, and R.C. Jones, Phys. Rev. Lett. **36**, 1217 (1976).

[20] Traditionally, schematic MCT deals with a one time correlator, which, in our framework, is to be identified by C_{nn} at equilibrium, normalized by its equal time value: $\phi_{MCT}(t-t') = C_{nn}(t-t')/C_{nn}(0)$.

[21] E. Lippiello and M. Zannetti, Phys. Rev. E **61**, 3369 (2000).

[22] A. Coniglio, J. Phys. France **3**, C1-1 (1993); Nuovo Cimento D **16**, 1027 (1994); Physica A **281**, 129 (2000); Physica A **266**, 379 (1999).